Proceedings of the 9th International Conference on Cyclotrons and their Applications
September 1981, Caen, France

# THE MILAN SUPERCONDUCTING CYCLOTRON PROJECT

E.Acerbi, F.Aghion, F.Alessandria, G.Baccaglioni, G.Bellomo, C.Birattari, C.De Martinis, E.Fabrici, C.Pagani, F.Resmini, L.Rossi, A.Salomone, L.Serafini, L.Troiano, G.Varisco, V.Venturini.

University of Milan, Milan, and Istituto Nazionale di Fisica Nucleare, Milan, Italy.

Abstract.- This paper presents the main characteristics of the Milan superconducting cyclotron, now under construction, and the actual project status.

1. Introduction.- The construction of the Superconducting Cyclotron at the University of Milan, funded by the Italian National Institute for Nuclear Physics (I.N.F.N.) is presently underway, after final authorization for the go-ahead on the project was granted on Feb. 1981. During this year, many design features of the machine have been reviewed, and most major parameters frozen, as outlined in Ref (1).

Procurement of major components has been initiated, while for others prototypes are being built.

It is the purpose of this paper to present the main features of the accelerator, and its current status. Since a few papers on detailed aspects of the design are given elsewhere at this Conference,[2-6] the emphasis will be more on a broad overiew of the project, and a discussion of the rationale for the various choices which have been made.

2. Main design features.- The machine is a three sectors, three dee, cyclotron with an effective K = 800, and a $K_{FOC}$ = 200. It was originally designed as a booster for a 16 MV Tandem and this capability remains as the main guideline of the project, the presently envisaged Tandem being the HVEC machine to be installed in Catania. The cyclotron will be equipped also with an internal ion source of the P.I.G. type, both for testing purposes and for the acceleration of very light ion beams ($H_2^+$, deuterons, alphas), for which such a source is fully adequate.

However, recent results in the development of high charge states heavy ion source, of the ECR and EBIS type, strongly suggest that the machine should also have an axial injection capability.

Feasibility studies[7] imply that such an injection is indeed possible with moderate (20 to 30 KV) injection voltages. It will therefore be implemented in this cyclotron, perhaps initially with an external P.I.G. ion source. No commitment, and in fact no funding request, has been made for any of the advanced ion sources now being developed at a number of Laboratories.

Using the Tandem as injector the cyclotron will have T/A vs A operating curves as shown in fig. 1. If operated with an external ion source, of the EBIS type, the maximum energy would be as shown in fig. 2. Expected intensities are of course still rather speculative at this time, for either Tandem, internal or external ion source combination. Our guesses are shown in fig. 2, together with the assumptions made.

The ions energies are shown in fig. 3, as a function of the accelerating frequency, for the four harmonics 1st, 2nd, 3rd, 4th which are deemed possible. An operating range of 15 to 48 MHz has been chosen,

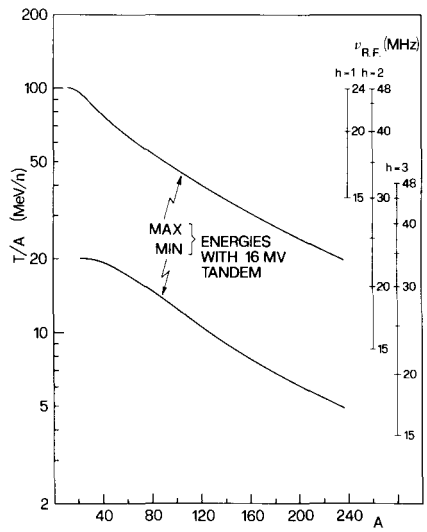


Fig.1 - Energy per nucleon Vs. ion mass number for coupled Tandem + Cyclotron operation.

the rationale being the possibility of obtaining in just one harmonic mode, h=2, all energies between 100

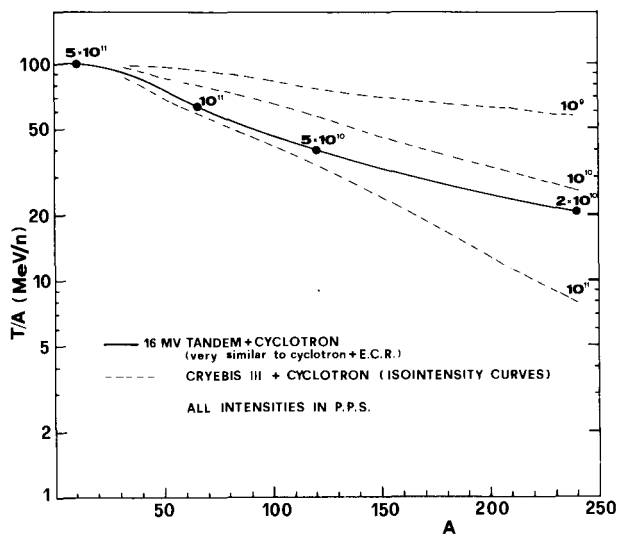


Fig.2 - Guessed intensities for:- Tandem + Cyclotron operation - a CRYEBIS III external source.

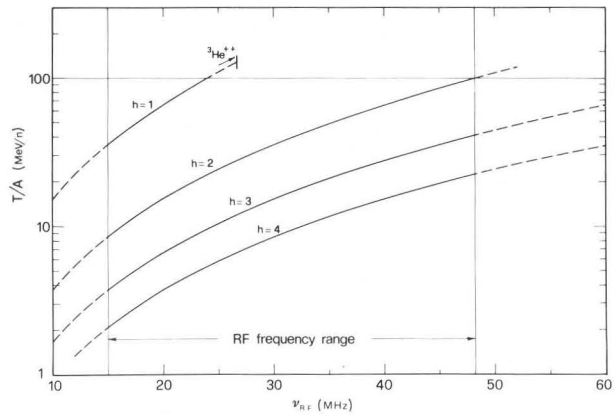


Fig.3 - Ions energy vs. R.F. frequency for the different harmonic modes listed.

MeV/n and 8 MeV/n. The operating diagram in the ($B_o$, Z/A) plane, i.e. the center field value and ion charge state, is presented in fig. 4. The bending and focusing limits, together with constant energy/nucleon lines, are shown. A few comments:

- we have tried to achieve the widest operating range, in terms of magnetic field, compatible with full saturation of the iron and the limits posed by the $\nu_R + 2\nu_z = 3$ resonance, discussed later. We found that a minimum operating field $B_o$ = 22 kgauss possible.
- this allows a variation of more than a factor of two in energy for Z/A = .5 ions, and also the acceleration, albeit in a restricted range of energies, of $^3He^{++}$, as shown in the figure.
- protons can only be produced via acceleration and extraction of $^2H^+$, and subsequent stripping.
- a minimum charge state Z/A = .05 is assumed. This is not so much for direct use of these beams, since their energies are ~ 2 MeV/n, but just to have a potential capability for the machine as injector.

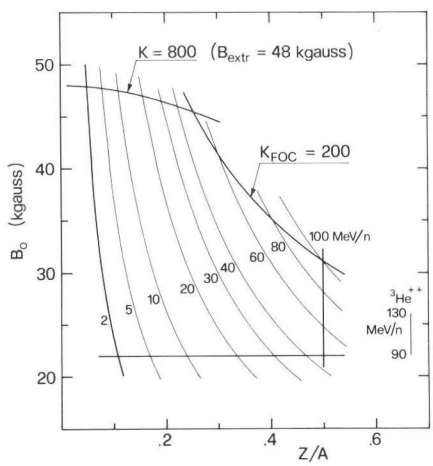


Fig.4- Operating diagram in the ($B_o$, Z/A) plane.

The major machine parameters are listed in Table I.

TABLE I - CYCLOTRON PARAMETERS

| | | |
|---|---|---|
| Bending limit | K | = 800 |
| Focusing limit | $K_{FOC}$ | = 200 |
| Pole diameter | | = 180 cm |
| No. of sectors | | = 3 |
| Average spiral constant | | = 1/45.7 rad/cm |
| Min. hill gap | | = 8.6 cm |
| Max. valley gap | | = 91.6 cm |
| Main coils Ampereturns | | = 6.55 $10^6$ at 3500 A/$cm^2$ average |
| Min. coils dist. from med. plane | | = 6.2 cm |
| Min-max center field | | = 22 - 48 kgauss |
| No. of trim coils | | = 20 |
| Max current in trim coils | | = 400 A |
| No. of Dees | | = 3, in valleys |
| R.F. range | | = 15 to 48 MHz |
| Operating harmonics | | = 1, 2, 3, 4 |
| Peak dee voltage | | = 100 KV |

3. Magnet structure.- A vertical cross section of the accelerator is presented in fig. 5, while a median plane sketch is shown in fig. 6.

The yoke, made of 5 cast steel pieces, has only minor variations with respect to what reported in (1). The "window" between poles and yoke which accomodates the coils, cryostat etc. has been somewhat increased

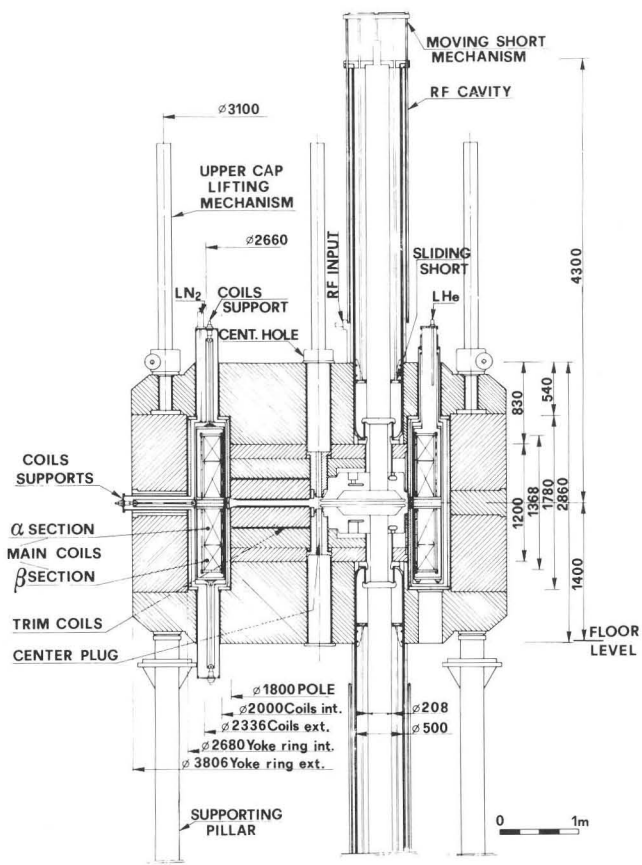


Fig.5- Vertical cross section of the cyclotron. All dimensions are in mm.

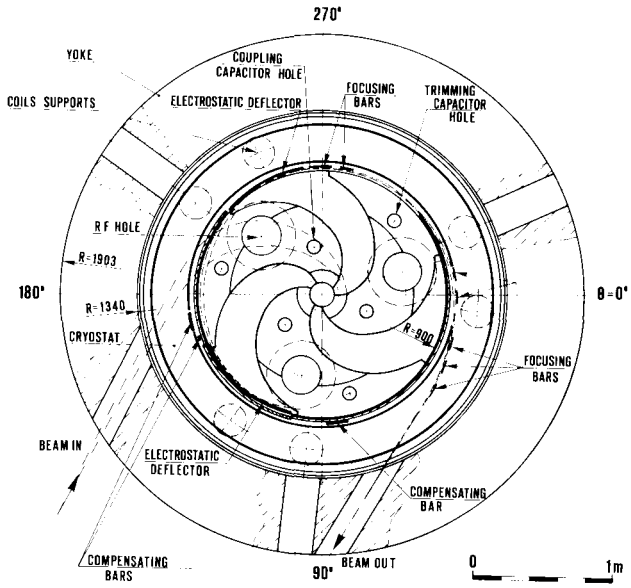


Fig.6 - Median plane sketch of the cyclotron.

and has now a radial width of 44 cm, and a total axial height of 178 cm. Also the outer shape of the yoke has been slightly changed. The poles, which form a single piece with the yoke caps, extend to 60 cm from the median plane. A 14 cm thick plate supports the sectors and valley shims, and is bolted to the pole as shown in fig. 5. The yoke parameters are listed in Table II.

TABLE II - YOKE PARAMETERS

| | |
|---|---|
| Pole radius | = 90 cm |
| Yoke inner radius | = 134 cm |
| Yoke outer radius | = 190,3 cm |
| Yoke full height | = 286 cm |
| Lifting range of upper cap | = 2 m |
| Steel = cast, carbon content | $\lesssim$ 0.01% |
| Total weight (incli sectors) | = 176 tons |

Since the attractive force between the poles at full excitation is around 2500 tons, deformations of the yoke are anticipated. These effects, given the number and positions of various holes,are difficult to calculate and therefore a 1:10 scale model has been built. The model has been subjected to a compression scaled according to analytical formulas, and the deformations measured. The data show that the yoke should have a axial deformation less than 0.3 mm, by large margins well within elastic limits.

The sectors are 33° wide at the radius of 9 cm., where they begin, and increase linearly in width up to 46° at R = 40 cm. This width stays constant thereafter up to R = 72 cm, the average spiral constant being 1/45.7 rad/cm. From then on the sectors width increases reaching 52° at R = 86.7 cm. This is done in order to match the field produced by the iron to the requirements for minimum trim coil power[8]. The spiral constant also increases in this region, reaching 1/31.4 rad/cm at R = 86.7 cm, in order to improve the axial focusing. From R = 86.7 cm to R = 90 cm the sectors are radial, to decrease the axial focusing frequency $\nu_z$, in the region where the $\nu_R + 2\,\nu_z = 3$ resonance limits the machine performance.

As shown in fig. 7, the hills are split into two parts, in order to wind the twenty trim coils around the upper part. Shims of proper height are place in the valleys, to produce the desired average field shape. The last shim, positioned between R = 87.5 cm. and R = 90 cm, which extends up to 12.5 cm from the median plane, will actually be machined as a single ring, for better mechanical stability, and fitted around the pole as shown in fig. 7. Also a 2.5 cm thick ring, which is actually the inner wall of the vacuum tank, extends up to 6.0 cm from the median plane, to limit the fringing field decrease. It has a clearance, with respect to the pole, of 6 mm.

Because of inferior costs and easier mechanical assembly, all the sectors and valley shims will be machined with a numerically controlled milling machine. Thus each sector will be manufactured in just one piece. The sectors will be rounded at the edges with a 20 mm radius of curvature, in order to facilitate the winding of the trim coils.

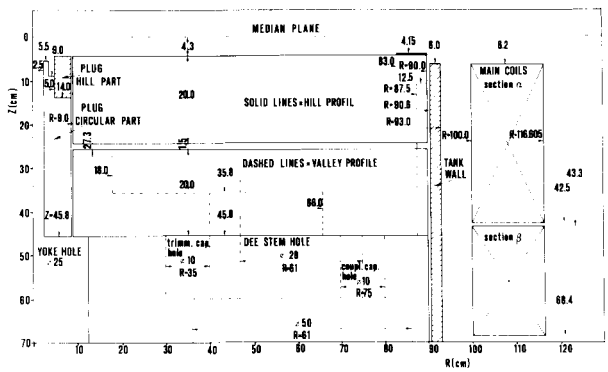


Fig.7- Hill and valley radial profiles. All dimensions in cm.

As shown in figs 5 and 7 a center hole of 5 cm diameter is provided either for the insertion of the internal ion source or for axial injection purposes. The hole increases to a 25 cm diameter through the pole and the yoke to provide more room for devices needed for the axial injection (buncher, deflectors). A center plug, consisting of a cylindrical part and a hill part, as shown in fig. 7, compensates the hole effect on the magnetic field.

The twenty trim coils will be of the type already developed at MSU[8]. Each coil has two layers of 5 turns each, of 6x6 $mm^2$ conductor and carries a maximum current of 400 A. The last one has one layer only, in order to provide more space for the electrostatic deflector, which, for low fields, must slide sensibly inward. The main difference with respect to the MSU design is that our trim coils will have entrance and exit leads through the same hole on the side of the hill and are grouped in pairs. Four leads go therefore through the same hole, which has a diameter of 3 cm. This reduces considerably the number of holes, which are arranged as show in fig. 8. Other holes, besides those for the trim coils, are the central one, those for the R.F. dee stems, coupling and trimming capaci-

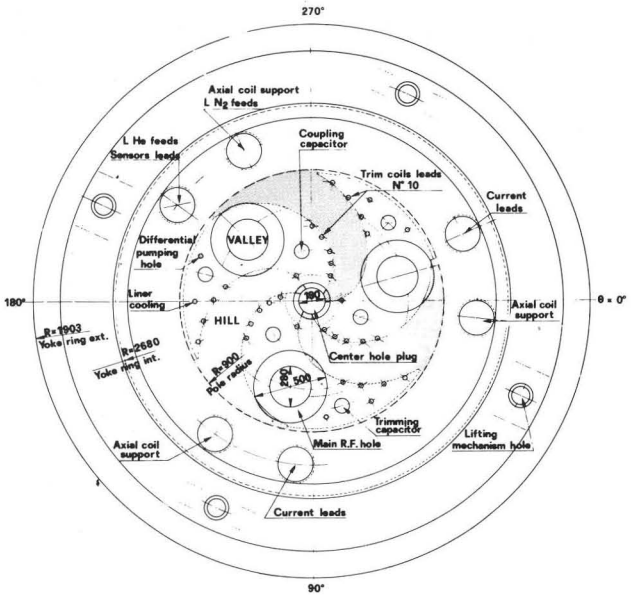


Fig.8- Sketch of the magnet from the top.

tor, (10 cm Ø) and those for pumping in the differential vacuum chamber constituted by the liner, which encloses the trim coils, and for the liner cooling.

4. The superconducting coils.- The main coils, whose cross sections is shown in detail in fig. 9, will be in a liquid helium bath. Their main characteristics are listed in Table III. They are split into two sections, $\alpha$ closer to the median plane and $\beta$ farther away, independently excited for isochronising the total average field. Since many details on the coils design and manufacturing technique are given in (2) here we just outline the main problems and solutions envisaged.

TABLE III - MAIN COILS PARAMETERS

| | |
|---|---|
| Max Amperturns | = 6.55 $10^6$ at 3500 A/cm$^2$ average density |
| Internal radius | = 100 cm |
| External radius | = 116.8 cm |
| Height of section $\alpha$ | = 36.4 cm |
| Height of section $\beta$ | = 25.2 cm |
| No. of turns | = 38 |
| Layers in $\alpha$ section | = 2 x 13 |
| Layers in $\beta$ section | = 2 x 9 |
| Min. distance from med.plane | = 6.2 cm |
| Cable type: | NbTi, monolithic insert in Cu cable 20 : 1 ratio |
| Cable dimensions | = 13. x 3.5 mm$^2$ |
| Insert dimensions | = 1.8 x 3.6 mm$^2$ |
| Max. nominal current | = 1944 A. |
| Total conductor length | = 22.60 km |

The currents needed in the $\alpha$ and $\beta$ sections, in order to produce an isochronous field for all ions and energies have been computed. The corresponding operating diagram is shown in fig. 10, where constant $B_o$ and Z/A lines are also plotted. The diagram shows that while $J_\alpha$ is always positive, between 1500 A/cm$^2$ and 3500 A/cm$^2$, $J_\beta$ must go from + 3500 A/cm$^2$ to - 1500 A/cm$^2$. This peculiar behaviour requires a careful analysis of the forces and stresses on the coils. Two limiting cases have been identified: a) $J_\alpha = J_\beta = 3500$ A/cm$^2$, b) $J_\alpha = 3000$, $J_\beta = -1500$ A/cm$^2$.

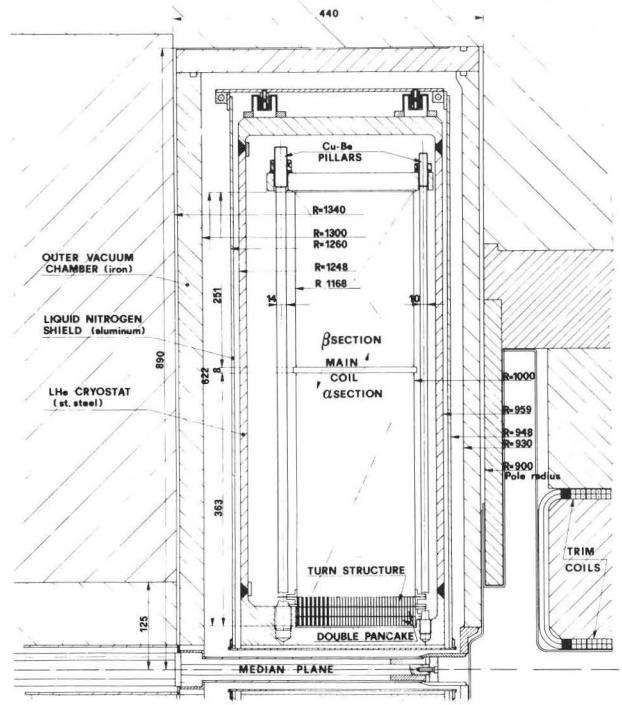


Fig.9- Main coils cross section

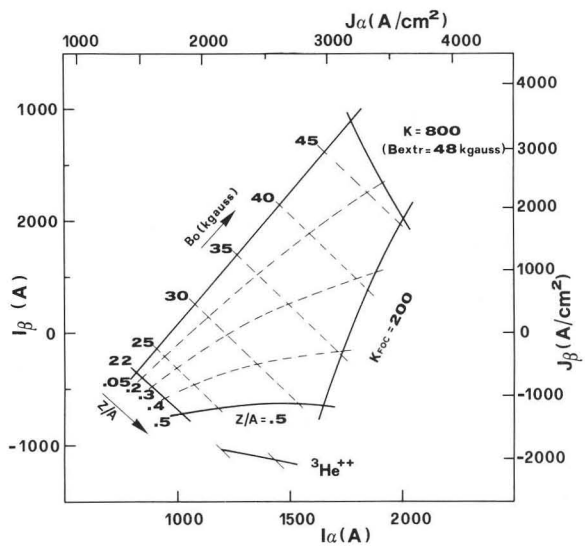


Fig.10- Cyclotron operating diagram in the ($I_\alpha$ , $I_\beta$) plane.

In the first case, both sections are attracted toward the median plane, with a total force of 1600 tons, and both tend to expand radially. In the second, the $\beta$ section is pushed away from the median plane with ~ 600 tons, while the $\alpha$ section is still attracted

toward it with ~ 100 tons. The stresses are of radial compression in the $\alpha$ section, and expansion in the $\beta$ section. It is this peculiar regime of forces which led us to the solution envisaged in fig. 9. Rods disposes around the inside and outside of the coils are prestressed, at room temperature, with ~ 700 tons. They will thus exert a net force toward the median plane also in the second case, in order prevent a coil lift-off. More details are given in (2).

The coils will be wound with the double pancake technique and consist of 38 turns with 26 layers in the $\alpha$ section and 18 layers in section $\beta$. Conductor data are listed in table I.

At the average max current density of 3500 A/cm$^2$ the current will be 1944 A. Three current leads are used for exciting both sections, so that the center "tap" common to the $\alpha$ and $\beta$ sections carries either the current difference between the $\alpha$ and $\beta$ sections, if they are both positive, or their sum when the signs are opposite.

The main features of the cryostat, liquid nitrogen shield and vacuum chamber are also shown in fig.9, while more details can be found in (2). A consumption of 15 l/h. of LHe, and 15 W is anticipated.

5. Magnetic field properties and beam dynamics.- The field produced by the magnet structure just discussed looks excellent. The average field has been calculated using the Poisson program and a model similar to that employed at MSU[9] over a grid of 23 values in the ($J_\alpha$ , $J_\beta$ ) plane which covers the whole operating range. The Poisson grid is shown in fig. 11, where the different iron fractions used to simulate hills, shims, and holes are also listed.

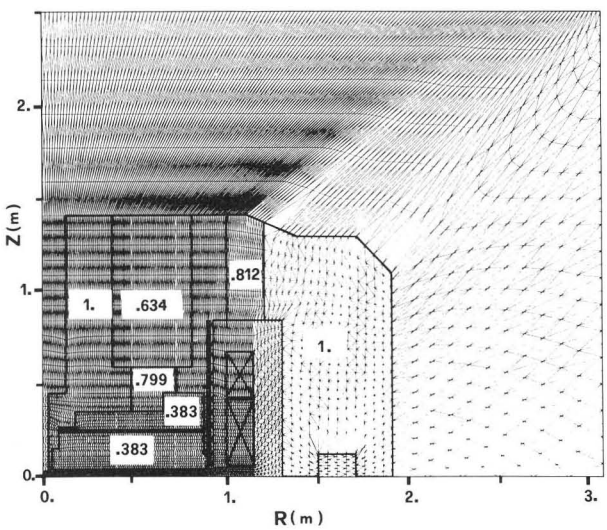


Fig.11- Poisson grid used for magnetic field calculations.

The average field produced by the iron is plotted in fig. 12 at 4 different excitations including the highest and lowest ones. With this field, isochronism can be obtained for all ions with modest trim coils currents. A diagram of the limiting current values, for each of the 20 trim coils, is presented in fig. 13.

Flutter, as calculated by the uniform saturation approximation, provides adequate focusing. As an example, fig. 14 presents the working path in the ( $\nu_R$,

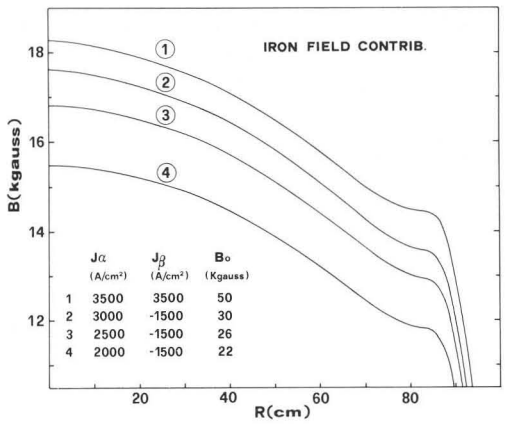


Fig.12 - Average magnetic field at four different main coils excitations.

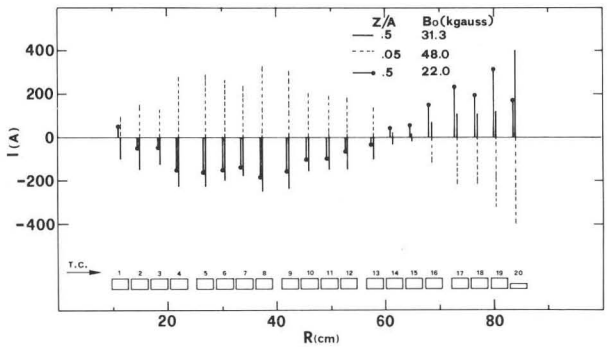


Fig.13 - Limiting current values for the 20 trim coils

$\nu_Z$) plane for 100 MeV/n and 40 MeV/n fully stripped light ions. The minimum $\nu_Z$ is about .18 which leaves a considerable margin.

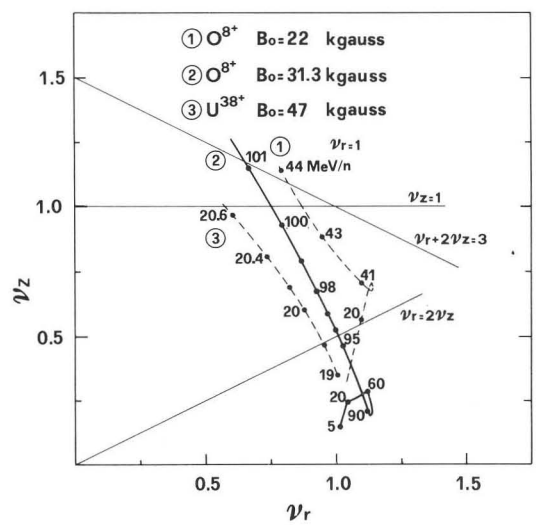


Fig. 14- ( $\nu_R$, $\nu_Z$) working path for the 100 MeV/n and 40 MeV/n fully stripped ions, and 20 MeV/n uranium ions.

The $\nu_R + 2\,\nu_Z = 3$ resonance, which cannot be crossed, moves inward the lower the magnetic field. This is shown in fig. 15, where the crossing of said resonance is plotted as a function of the equilibrium orbit radius for the Z/A = .5 ions at various center field values. This is the only drawback of the 3- sector configuration and requires a radial movement of the extraction system spanning 2.5 cm, as will be seen later.

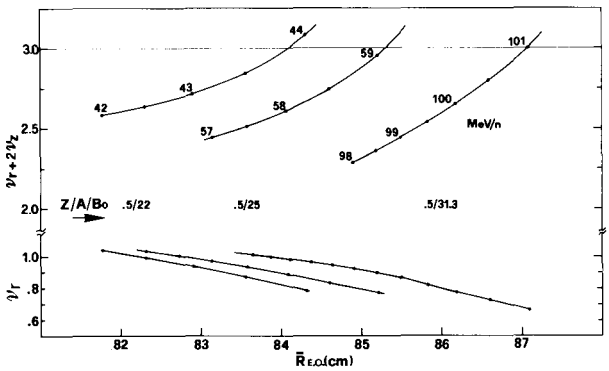


Fig.15 - ( $\nu_r + 2\,\nu_Z$) and $\nu_R$ values as a function of the equilibrium orbit radius for fully stripped light ions at minimum and maximum fields.

More details on the magnetic field properties can be found in (3). The degree of confidence in the magnetic field calculations, also after the M.S.U. experience[9], is high enough so that we shall machine all necessary penetrations in the cryostat, for extraction and injection purposes, at construction time i.e. before magnetic field measurements are available.

6. Injection, extraction.- Injection from the Tandem originates from a common point at 2.5 meters from the magnet center, visible in fig. 6. A steering magnet at that point provides a $\pm$ 1.5° deflection needed to match the required injection path for all particles and energies. Stripping occurs in a hill, the radial range being between 9 and 21 cm, with both azimuth and radius of the stripping foil being adjustable. The beam behaviour through the injection path looks very reasonable. The radial and axial phase spaces for the 100 MeV/n case are shown, at several radii, in fig.16.

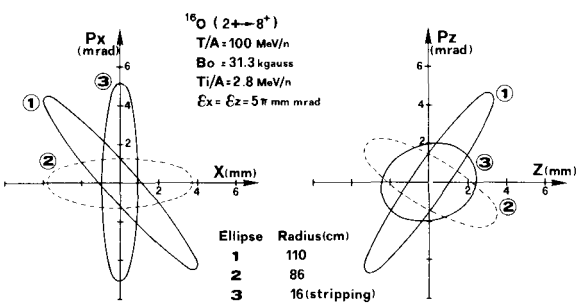


Fig.16 - Radial and axial phase space of injected beams at various radii along the injection trajectory.

This phase space is matched, at the stripping position, to the cyclotron eigenellipse, for an assumed emittance of 15 mm x mrad in both planes. The need for a magnetic channel, perhaps an active superconducting one in the yoke traversal in order to ease the matching conditions for the external beam line, is now investigated.

As seen in fig. 6, extraction is accomplished by two electrostatic deflectors, the first one 52° long and the second 40° long, positioned in two consecutive hills. They are followed by 7 magnetic channels, of the passive type, which provide both field bias and a focusing gradient. The main parameters of the extraction system elements are listed in Table IV.

TABLE IV - EXTRACTION ELEMENTS PARAMETERS

| Element | $\vartheta_{in}$ | $\vartheta_{fin}$ | E (kV/cm) | $\Delta$B (kG) | $\partial B/\partial x$ (kG/cm) |
|---|---|---|---|---|---|
| E1 | 104 | 156 | 140 | --- | --- |
| E2 | 222 | 262 | 140 | --- | --- |
| M1 | 264 | 274 | --- | -2. | 3.86 |
| M2 | 278 | 284 | --- | -1.8 | 2.12 |
| M3 | 348 | 354 | --- | -1.2 | 3.63 |
| M4 | 358 | 364 | --- | -1.2 | 3.63 |
| M5 | 378 | 384 | --- | -1.2 | 3.63 |
| M6 | 388 | 394 | --- | -1.2 | 3.63 |
| M7 | 398 | 404 | --- | -1.2 | 3.63 |

The compensation of the 1st harmonic produced by the channels is made via three additional bars, also visible in fig. 6. Compensation down to less than a gauss can be achieved near the $\nu_R = 1$ resonance crossing. More details can be found in ref. 4.

All elements must be radially movable by about 2.5 cm, as explained earlier. Furthermore, due to the large range of magnetic fields and henceforth the sizable variation in orbits scalloping, the shape of the electrostatic deflectors must change slightly in order to fit all extraction trjectories. Each deflector will therefore consist of two parts, which can rotate around each other. The splitting occurs at about the center of each deflector. A sketch of a prototype now being built is shown in fig. 17.

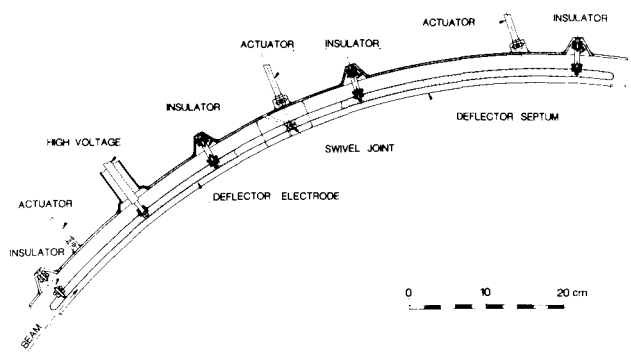


Fig.17 - Sketch of a prototype for the electrostatic deflectors.

The beam is well confined along the extraction path. As an example, fig. 18 shows the radial and axial beam envelopes for a 5.6 mm x mrad emittance, at 100 MeV/n. A detailed treatment of beam dynamics prior to extraction, and extraction optics, is given in (4).

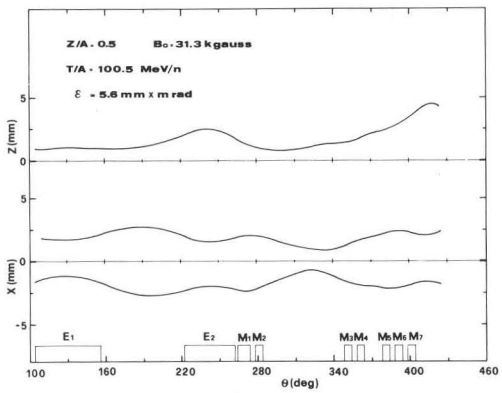


Fig.18 - Radial and axial envelopes of a 100 MeV/n extracted beam.

7. R.F. system-Vacuum.- As shown in fig. 5, the present design of the R.F. system calls for a cavity which is in air for the whole length of the short circuit movement. Connection between air and vacuum is made with an insulator, now being designed, in a way qualitatively similar to that adoped for the K800 at MSU. The rationale for this choice was the concern about mechanical instabilities of the cavity due to thermal gradients, vibrations etc. In this sense the mechanical constraint provided by the insulator gives a lot of safety.

It is anticipated that, even with the new design, the necessary power will not exceed 75 KW. According to our last calculations, the power, together with the short circuit current density in A/cm, and the distance of the short circuit from the median plane are plotted as a function of R.F. frequency in fig. 19. It has not been decided, yet, whether to use pushing rods, or some other device, in order to drive the short.

The dees will contain the panels for pumping. A cacuum of $1 \times 10^{-7}$ torr is, in principle, required. While the most likely solution is the use of cryopanels, of the two-stage type, we are also investigating the possible use of getters.

More details on the R.F. system, and the mechanical structure of the cavities, are reported in Ref. 5.

8. Project status.- As of this date, the following major components have been ordered:

- magnetic yoke and iron for the sectors, to Hoesch, Dortmund, (Germany).
- R.F. power amplifiers, to Brown Boveri, Bade, Switzerland.
- helium liquifier to Sulzer, Switzerland, model TCF 100 with just one compressor, with a capacity of 30 l or 80 watts, per hour.
- superconducting cable, to La Metalli Industriale, Florence, Italy.
- main coils winding, which will be executed by Ansaldo, Genoa, Italy.

The main coils power supply is being built in the house. We have also on construction: a prototype of sectors and a full trim coils set; a full scale prototype of the electrostatic deflectors to be tested in the present Milan cyclotron; several prototypes of minor components, mainly related to the main coils(e.g. the rods for stacking the pancakes etc.).

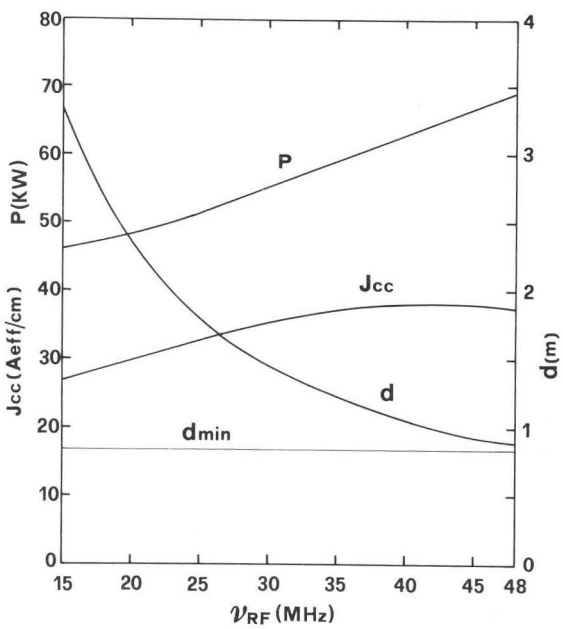


Fig.19 - Power, current density and distance from the median plane of the short circuit as a function of the R.F. frequency.

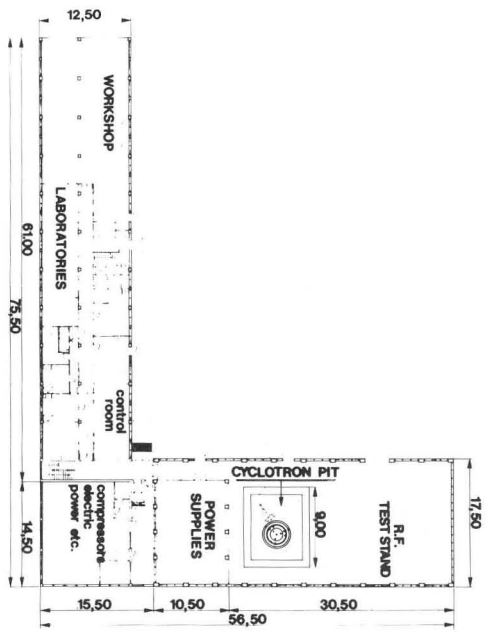


Fig.20 - Plan of the new building.

Elements of the magnetic field measurements system are being tested. The electronics, computer PDP 11/44 etc. are also on procurement. Some of these components will be the testing ground for the computer control of the machine.

A new building will be needed for the cyclotron, as well as a new one for laboratories, offices, etc. A sketch of the envisaged plan is shown, in a self-explanatory way, in fig. 20. The cyclotron building will have 650 $m^2$ of space, while for offices etc. we shall have 2100 $m^2$, distributed over three floors. It is expected that construction, once exhausted all formalities, may begin at the end of this year.

References

1. E. ACERBI et al., IEEE Transaction on Nuclear Science, NS 28 (1981) 2095.
2. E. ACERBI, F. ALESSANDRIA, G. BACCAGLIONI and L. ROSSI, Design of the Main Coils for the Milan Superconducting Cyclotron, paper presented at this Conference.
3. G. BELLOMO, C. DE MARTINIS and L. SERAFINI, Design of the Magnetic Field for the Milan Superconducting Cyclotron, paper presented at this Conference.
4. E. FABRICI and A. SALOMONE, The Extraction System for the Superconducting Cyclotron at the University of Milan, paper presented at this Conference.
5. C. PAGANI, G. VARISCO, V. VENTURINI and ALESSANDRIA, The Milan Superconducting Cyclotron RF Design, paper presented at this Conference.
6. F. AGHION, C. RIVOLTELLA and L. TROIANO, Outline of the Control System for the Milan Superconducting Cyclotron, paper presented at this Conference.
7. G. BELLOMO, F. MARTI and F. RESMINI, Feasibility of Axial Injection in Superconducting Cyclotrons, to be published by Nuclear Instruments and Methods.
8. G. BELLOMO and F.G. RESMINI, Nuclear Instrulents and Methods, 180 (1981) 305.
9. G. BELLOMO, D.A. JOHNSON, P. MILLER and F.G. RESMINI, Nuclear Instruments and Methods 180 (1981) 285.

" DISCUSSION "

P. LAPOSTOLLE : Can you say something about the cost of your machine ?

F. RESMINI : As estimated today, the cost is about $ 6 millions. This of course does not include building or personnel costs.

J.A. MARTIN : When do you expect the first beam ?

F. RESMINI : Present schedule anticipates machine tests in 1985, sometime in Spring. Whether this schedule can be maintained depends upon a lot of factors, as you know, too well. We hope not to have a kind of regular financing, but of course it is really too early to make any sensible predictions.

Mrs H. MATHIEU-FARAGGI : Difference between cryogenic separated sectors and compact cyclotrons with respect to performance, cost, best domain of utilization ?

F. RESMINI : It looks like in the range up to K$\sim$1000 and energies, for fully shipped light ions, up to $\sim$ 200 MeV/n, there is really no advantage in going to cryogenic separated sector machines. For much higher (300-400 MeV/n) light ion energies, the separated sector machines may offer a way of overcoming some limitations of compact cyclotrons (resonances etc..) although with a very steep cost increase.

W. SCHOTT : A superconducting separated sector cyclotron has larger dimensions than a superconducting compact one. This is due to the wide free spaces between the sector magnets. These open spaces, which can be used to implement high shunt impedance cavities, do not necessarily raise the costs. However, because of the lower mean field, the total weight of a separated sector machine is certainly larger and costs more than the compact type, if only the K-bending-factor is taken into account. This factor does not describe the final energy of light ions in the case of the compact cyclotron. Therefore, a simple statement on the costs is difficult to make.